Mechanics of Materials 187 (2023) 104846

Contents lists available at ScienceDirect

Mechanics of Materials

journal homepage: www.elsevier.com/locate/mechmat

Research paper

Use of hardness, PIP and tensile testing to obtain stress-strain relationships for metals

T.J.F. Southern [a], J.E. Campbell [a], C. Fang [a], A. Nemcova [b], A. Bannister [b], T.W. Clyne [c,a,*]

[a] Plastometrex Ltd204 Science Park, Milton Road, Cambridge, CB4 0GZ, UK
[b] HSE Science and Research Centre, Harpur Hill, Buxton, Derbyshire, SK17 9JN, UK
[c] Department of Materials ScienceUniversity of Cambridge, 27 Charles Babbage Road, Cambridge, CB3 0FS, UK

ARTICLE INFO

Keywords:
Hardness
Indentation plastometry
Stress-strain curve
Tensile testing

ABSTRACT

Both hardness testing and Profilometry-based Indentation Plastometry (PIP) can be used to obtain features of (tensile) stress-strain curves. The two tests are superficially similar, involving penetration (under a known load) of an indenter into the flat surface of a sample, followed by measurement of dimensional characteristics of the residual indent. The associated data handling procedures, however, are very different in the two types of test. Hardness numbers, which are commonly based on measurement of the lateral extent or depth of the indent, essentially give a semi-quantitative indication of the resistance to plastic deformation: going beyond this to infer features of the (nominal) stress-strain curve – notably the yield stress (YS) and Ultimate Tensile Stress (UTS) – can only be done via empirical correlations (often restricted to certain types of alloy). PIP testing, on the other hand, involves measurement of the complete indent profile, followed by (automated) iterative FEM modelling of the indentation, allowing the complete (true) stress-strain curve to be obtained. This paper covers application of both approaches to 12 different alloys, with inferred stress-strain characteristics being compared with those from tensile testing. Insights are provided relating to the very different levels of detail and reliability offered by the two procedures.

1. Introduction

Obtaining well-defined information about the plasticity response of metals continues to be of major industrial and scientific importance. By far the most convenient and versatile of the techniques currently in widespread use is that of hardness testing. There are several hardness measurement schemes, each giving different numbers, but the idea is the same for most of them. A specified load is applied to an indenter, which penetrates into the specimen, causing plastic deformation and leaving a permanent depression. A hardness number can be obtained in several ways, but the most common procedure involves measurement of either the indent lateral size (diameter or diagonal) or the penetration depth. The depth and shape of the depression depend on the load, the shape of the indenter and the response (hardness) of the specimen. Hardness is commonly defined as the force (load) divided by the area of contact between indenter and specimen (although this is not the case for all schemes). This ratio nominally has dimensions of stress, although it is usually quoted as simply a number (with units of kgf mm^{-2}). The most widely used test is the Vickers, which is based on a square pyramidal indenter, with the number being derived from the average of the two diagonals. This is usually obtained by viewing the indent in the optical microscope, although the exact outcome of this depends on the perceived locations of the "ends" of the diagonals (potentially influenced by focussing conditions etc). It has certain attractions, including the potential for use with a wide range of loads. It may be regarded as representative of the complete range of hardness tests.

In any event, the stress level that the hardness number represents bears no simple relation to the stress-strain curve of the material, or indeed to the stress field created in the sample. Different regions of the specimen are subjected to different plastic strain levels, ranging from zero (at the edge of the plastic zone) to perhaps several tens of %, or even well over 100% (close to the indenter, particularly the edges of "sharp" indenters). Even this maximum strain level is not well defined, since it depends on the indenter shape, the applied load and the plasticity characteristics. While the true stress-strain relationship of the material (von Mises stress as a function of equivalent plastic strain) does dictate the indent dimensions (for a given indenter shape and load), inferring the former from the latter is not straightforward and no attempt is made

* Corresponding author. Department of Materials ScienceUniversity of Cambridge, 27 Charles Babbage Road, Cambridge, CB3 0FS, UK.
E-mail address: twc10@cam.ac.uk (T.W. Clyne).

https://doi.org/10.1016/j.mechmat.2023.104846
Received 15 May 2023; Received in revised form 20 October 2023; Accepted 23 October 2023
Available online 27 October 2023

to do this in conventional hardness testing. Typical numbers obtained for a given material using different types of (indentation) hardness tests are significantly different. This is unsurprising in view of the dependence of the plastic strain field on the indenter shape and the applied load. One of the issues with hardness testing is that, since the load does tend to affect the hardness number, it should always be provided when quoting one (but often is not). In the case of Vickers hardness, it is sometimes assumed that the load is 10 kg if it is not explicitly stated.

Nevertheless, there is a strong incentive to relate hardness numbers to the genuine plasticity characteristics of the metal (captured in the form of the true stress-strain relationship). Ideally, this is the true von Mises stress as a function of the true von Mises ("equivalent plastic") strain, although it is common to distil two values from this – the yield stress (YS) and the ultimate tensile strength (UTS). The latter is the nominal stress level at which necking starts in a tensile test (assuming that it is not interrupted by premature fracture, which can happen with very brittle metals). Both the YS and the UTS (dictated by necking) can be obtained from the true stress – true strain curve, using well-established analytical relationships - see §3.1 below. It is clear that there is no possibility of a rigorous derivation of these properties from a hardness number, but there have been many attempts (Tekkaya, 2001; Umemoto et al., 2001; Busby et al., 2005; Pavlina and Van Tyne, 2008; Hashemi, 2011; Tiryakioglu, 2015; Sandomirskii, 2017; Matyunin et al., 2021; Pintaude, 2022; Chen and Cai, 2018) to rationalise hardness data in various ways and often to identify empirical analytical relationships (based solely on experimental data). Some such equations have been incorporated into standards published by bodies such as ASTM and BSI. They are usually expressed only in the form of YS and UTS values, with no attempt made to obtain a full stress-strain curve from a hardness number. Most of the proposed relationships are simple linear correlations, with or without some kind of offset – i.e. the equations used (with Vickers hardness numbers) are generally of the form:

$$\mathrm{YS} = \frac{H_\mathrm{V}}{A} + \mathrm{C} \tag{1}$$

$$\mathrm{UTS} = \frac{H_\mathrm{V}}{a} + \mathrm{c} \tag{2}$$

where C and/or c (with units of MPa) may or may not have a value of zero and H_V is also expressed in MPa (obtained on multiplying the value in kgf mm^{-2} by a factor of g). The parameters A and a are thus dimensionless numbers.

It is widely accepted that errors are likely to arise if an attempt is made to identify parameter values that are universally applicable and in most cases they refer to some kind of class or sub-class of alloy. For example, Pavlina and Van Tyne (Pavlina and Van Tyne, 2008) proposed (based on data for a large number of non-austenitic, hypo-eutectoid steels) the values for these four parameters shown in Table 1. In slight contrast to this, Umemoto et al. (2001) (also after examining data for a large number of steels of the same type) suggested that C and c should be zero, but that the values of A and a should be adjusted depending on the sub-class within this broad category of steel. These values are also shown in Table 1. Many other variants have been proposed, but these two formulations are typical of them.

Table 1
Proposed best-fit values (from extensive experimental data) of the parameters in Eqns. (1) and (2), for non-austenitic, hypoeutectoid steels (sub-divided or not).

Source	Class of Metal	Parameters for YS (Eqn. (1))		Parameters for UTS (Eqn. (2))	
		A (−)	C (MPa)	a (−)	c (MPa)
Pavlina & Van Tyne (Pavlina and Van Tyne, 2008)	Non-austenitic, hypo-eutectoid steels	3.4	−90.7	2.6	−99.8
Umemoto et al. (Umemoto et al., 2001)	(i) Ferritic steels	5.79	0	3.97	0
	(ii) Pearlitic steels	4.90	0	3.27	0
	(iii) Bainitic steels	4.27	0	3.43	0
	(iv) Martensitic steels	5.31	0	3.08	0
	(v) Tempered martensitic	3.17	0	2.72	0

It may also be noted that correlations between a hardness number and YS/UTS values (and also between different hardness numbers) are proposed in certain standards, such as BS EN ISO 18265:2013. Most of these are restricted to certain categories of alloy. While these are sometimes presented as look-up tables, they are in most cases very close to being simple analytical (linear) relationships. For example, as shown in Fig. 1, this standard gives UTS values that are very close to the linear relationships shown. If the H_V values are expressed in MPa, then this relationship can be written in the same form as Eqn. (2):

$$\mathrm{UTS} = \frac{H_\mathrm{V}}{3.08} \tag{3}$$

This is similar to the relationships proposed by Umemoto et al. and indeed all such expressions have been obtained in much the same way – i.e. by fitting to large sets of experimental data. They all tend to give a value for the constant a of approximately 3.

In fact, even with limitations being imposed on the range of metals to which specific equations should be applied, the reliability of YS and UTS values obtained from hardness numbers in this way tends to be variable. It should also be emphasized that such equations are simply empirical correlations, with no attempt inherent in them to account for actual shapes of stress-strain curves or how this might affect the reliability. Nevertheless, certain points can usefully be noted. An important one is that, in the complete absence of work hardening - that is, for an "elastic – perfectly plastic" metal, the stress and strain fields during indentation (with a Vickers indenter shape) are well-defined (in terms of the yield stress) and universal. This concept dates back to the early work of Tabor, 1948, 1996. With no work hardening, there is in fact a defined (rigorous) relationship between H_V and YS, which is linear (with no offset – ie C is zero). The theoretical value of A in Eqn. (1), which is obtainable via FEM modelling of the indentation, is close to 3 (and is independent of load). Moreover, in the complete absence of work hardening, necking will tend to occur during a tensile test immediately after yielding, so the same expression will also give the UTS.

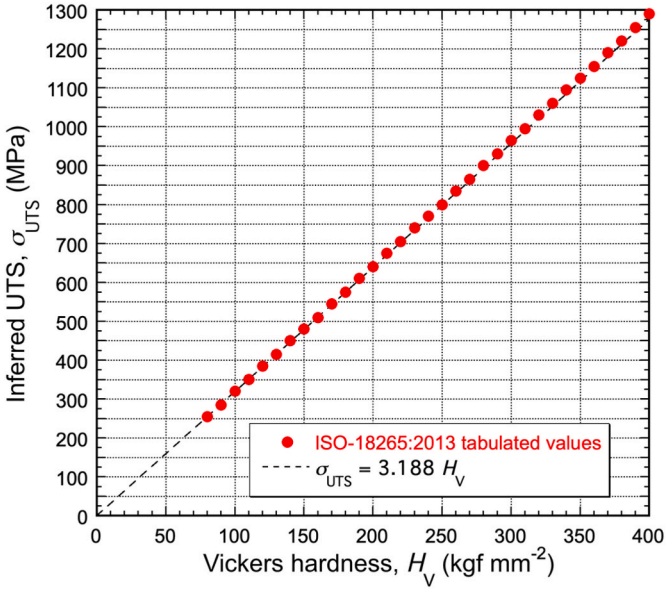

Fig. 1. Tabulated UTS values, plotted against H_V (with 10 kg load), according to the BS EN ISO-18265:2013 standard, together with a fitted linear relationship. These are taken from Table A1 in the standard (unalloyed steels, low alloy steels and cast steels).

It is evidently the work hardening that changes this picture dramatically. This is well understood – for example, see the discussion in Pintaude (2022). The problem is simply that, with no *a priori* information about the nature of the work hardening, it is difficult to predict on any rational basis either the YS or the UTS just from a hardness number: inherent in indentation is the fact that plastic strain levels vary with location and time throughout the test – when regions at the edge of the plastic zone are starting to yield, locations close to the indenter have already experienced large plastic strains. Unless work hardening is negligible, this introduces a large element of uncertainty. There have been many attempts (Tekkaya, 2001; Branch et al., 2010; Zhang et al., 2013) to take account of the effect of work hardening, some of them based on the idea of a "representative" strain, with or without the use of a strain hardening exponent – which of course is unknown if simply applying a hardness test to a sample. Tabor suggested (Tekkaya, 2001; Tabor, 1948, 1996) that the value of A should be 2.9 if there is work hardening, with a typical representative strain being 8%. It is in any event clear that such empirical correlations can only take some sort of averaged account of the different extents of work hardening within the class of alloy concerned.

In contrast to this complex situation regarding the relationship between a hardness number and the stress-strain curve, Profilometry-based Indentation Plastometry (PIP) allows it to be obtained directly from local regions. This methodology is conceptually simple and rigorous, but the development of commercially viable stand-alone products has required optimisation of control and simulation software, linked to equipment for automated creation and characterization of suitable indents. The procedure is that of iterative FEM simulation of the indentation (Kucharski and Mroz, 2007; Heinrich et al., 2009; Dean et al., 2010; Patel and Kalidindi, 2016; Dean and Clyne, 2017; Chakraborty and Eisenlohr, 2017; Campbell et al., 2018; Meng et al., 2019; Xue et al., 2020; Frydrych and Papanikolaou, 2022), converging on the stress-strain relationship (captured in a constitutive law) that gives optimal agreement between measured and modelled outcomes. It has also been shown (Lee et al., 2009; Yao et al., 2014; Wang et al., 2017; Campbell et al., 2019) that there are important advantages to using the indent profile, rather than the load-displacement curve, as the target outcome.

A further important advance has been the recognition that, if "scale-independent" stress-strain relationships are being sought, then the volume being deformed must be large enough to be representative of the bulk - which usually translates into it containing a relatively large number of grains. In most cases, "nano-indenters" are not suitable for this. There are also certain other requirements, such as a need (Campbell et al., 2018; Clyne and Campbell, 2021) to create plastic strains in the range of up to at least a few tens of %. Recent work has covered application of the PIP technique to a wide range of materials and effects. These include study of welds (Gu et al., 2022), pipelines (Warwick et al., 2023), additively-manufactured components (Tang et al., 2021; Southern et al., 2023), metal matrix composites (Reiff-Musgrove et al., 2023), effects of residual stress (Burley et al., 2021), case-hardened layers (Ooi et al., 2022), very hard metals (Campbell et al., 2022) and porous metals (Reiff-Musgrove et al., 2022). There is also a review paper (Clyne et al., 2021) that summarises various aspects of the methodology.

The present work is focussed on comparing, for a representative set of a dozen materials, the outcomes of hardness-based and PIP-based testing procedures with those from conventional tensile testing. Interpretation of these results is assisted by FEM simulation of the tests. The hardness testing is limited to the Vickers procedure, although the results are expected to be equally applicable to other types of hardness test.

2. Experimental procedures

2.1. Materials

The (12) materials used in this work are listed in Table 2. They were selected with the aim of covering a wide range of plasticity characteristics. Furthermore, it was confirmed via various trials that all of these materials are at least approximately isotropic and homogeneous. It is therefore unnecessary to specify directions or locations for any of the tests.

Table 2
Metal codes, alloy types and forms for the materials tested. The elastic constants listed are approximate values used in the FEM simulations inherent in the PIP testing (and also applied to the Vickers hardness test).

Metal Code	Type of metal	As-received form	Young's modulus, E (GPa)	Poisson ratio, ν (−)
A	Waspalloy (Ni-superalloy)	Forged plate	200	0.33
B	Aluminium 7075	Rolled plate	70	0.33
C	Martensitic steel (0.38%C)	Forged block	200	0.33
D	Carbon steel (0.45% C)	Forged bar	200	0.33
E	316 L Stainless steel (~0.03%C)	Extruded rod	200	0.33
F	S355 Low alloy steel (0.23%C)	Rolled plate	200	0.33
G	4340 Low alloy steel (~0.4%C)	Extruded rod	200	0.33
H	Rail steel HP355 (~0.8%C)	Hot rolled rail	200	0.33
I	Rail steel R260 (~0.8%C)	Hot rolled rail	200	0.33
J	Plain C steel (0.14% C)	Mannesmann pipe	200	0.33
K	Copper (As-received)	Extruded rod	115	0.33
L	Copper (Annealed)	Extruded rod	115	0.33

2.2. Tensile testing

Tensile testing was carried out using an Instron 3369 loading frame. The samples were cylindrical, with a diameter of 5 mm, a reduced section length of 29 mm and a clip gauge length of 25 mm. All of the tests were repeated, but in general the reproducibility was high and just single stress-strain curves are presented here for each material. One issue with processing of the tensile data concerns evaluation of the two parameters that are commonly extracted – the YS and UTS. The UTS was simply taken as the largest (nominal) stress recorded during the test. For the YS, however, there is more uncertainty, particularly for curves that exhibit noticeably transitional yielding. In this work the 0.2% offset procedure was used.

2.3. Hardness testing

2.3.1. Testing procedure

Hardness testing was carried out using a Buehler Wilson VH3300 automatic Vickers hardness tester, with a load of 10 kg. Samples were in the form of small pieces, with a thickness of at least about 5–10 mm and lateral dimensions of the order of 10–20 mm. Surfaces for indentation were polished to at least 6 μm finish. The indent diagonal was taken to be the average of the two measurements (made via the built-in optical microscopy system). In general, these two diagonals were very close, reflecting the isotropy of these materials, and also their relatively fine grain structures – even with the harder materials, the indents still tended to straddle at least several grains. For each material, these measurements were repeated in 5 different locations.

The measured average diagonal length (d) was converted to a hardness number (load over contact area) using the standard equation, which is based on a simple geometrical construction for the specific shape of a Vickers indenter (a right square pyramid with an angle between opposite faces of 136°):

$$H_V = \frac{2F\sin\left(\frac{136}{2}\right)}{d^2} = 1.854\frac{F}{d^2} \tag{4}$$

where F is in kgf and the diagonal length, d, is in mm. In obtaining the contact area in this way, no account is taken of elastic recovery or of any "pile-up" (or "sink-in") around the indent.

2.3.2. FEM simulation of the test

The (changing) stress and strain fields generated during the test are relatively complex, but they can be accurately captured via FEM modelling (provided the true stress-strain relationship is known). This allows prediction of the indent shape, and hence of the hardness number likely to be obtained experimentally (making some assumption about how the diagonal length will be discerned in the optical microscope – the ends being at the peaks of the pile-ups is an obvious one). The mesh used for this work is shown in Fig. 2. It comprises 129,657 3D linear elements. A friction coefficient value of 0.1 was used in these simulations, although it was confirmed that its exact value has very little effect (unless it is set to zero, which does change the outcome significantly). Both indenter and sample are effectively semi-infinite in extent during these simulations.

2.4. Indentation Plastometry (PIP testing)

The PIP set-up used in this work has been described previously (Gu et al., 2022). The procedure, and various issues concerning its implementation, are fully detailed in a recent review paper (Clyne et al., 2021). Three steps are involved in obtaining a true stress-strain curve during a PIP test. These are: (a) pushing a hard spherical indenter into the sample with a known force, (b) measuring the (radially-symmetric) profile of the indent and (c) iterative FEM simulation of the test until the best fit set of (Voce) plasticity parameter values is obtained. The elastic constants (Young's modulus and Poisson ratio) are input data for the modelling, although their values have only a weak effect on the final outcome: the Young's modulus is only required to a precision of about ±10–15%, while the requirement for the accuracy of the Poisson ratio is even less demanding. Details of the mesh, boundary conditions etc are provided in several previous publications. For completeness, the Voce equation is reproduced here:

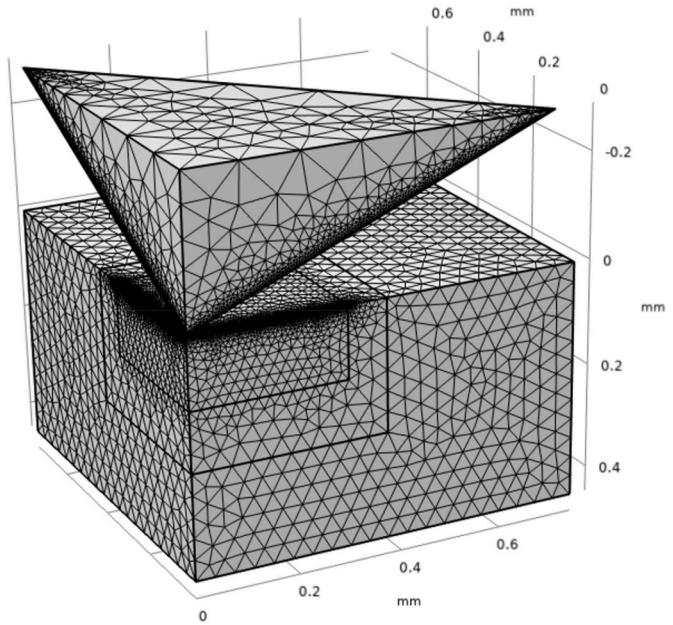

Fig. 2. FEM mesh used for modelling of the Vickers hardness test.

$$\sigma = \sigma_s - (\sigma_s - \sigma_Y)\exp\left(-\frac{\varepsilon}{\varepsilon_0}\right) \tag{5}$$

In addition to the yield stress, σ_Y, this expression includes the "*saturation*" stress, σ_s, and ε_0, which is a *characteristic strain* for the exponential approach of the stress towards this level. The stress is the von Mises stress and the strain is the von Mises (equivalent plastic) strain. Both are scalars.

The indenter was of Si_3N_4, with a radius of 1 mm. Sample preparation was the same as for the hardness testing. The penetration ratio (δ/R) was in the range 10–20%. Applied forces ranged up to about 6 kN. The indent topographies were characterized with a stylus profilometer having a resolution of about 1 μm. The indents had a diameter of ~1 mm. Several indents were made in each sample. The reproducibility was very high and a single representative profile was used in each case to obtain stress-strain relationships.

3. Test outcomes

3.1. Tensile testing

Results are shown in Fig. 3, as nominal stress – nominal strain plots. Also shown are corresponding curves for best-fit sets of Voce parameter values (listed in Table 3). These parameter sets define true (von Mises) stress – true (von Mises) plastic strain relationships (Eqn. (5)). Up to the onset of necking, they can be converted to nominal stress – nominal strain curves using the standard analytical relationships (based on conservation of volume during plastic deformation). Again for completeness, these relationships are presented here:

$$\sigma_T = \sigma_N(1+\varepsilon_N) \tag{6}$$

$$\varepsilon_T = \ln(1+\varepsilon_N) \tag{7}$$

where the subscripts N and T refer to nominal and true versions (and the conversion concerns only the plastic deformation – elastic deformation takes place in parallel with this). These equations allow conversion in either direction.

It is clear that these materials: (a) cover a wide range of plasticity characteristics, (b) have all been well-captured as (Voce-defined) true stress – true plastic strain relationships and (c) are all "well-behaved".

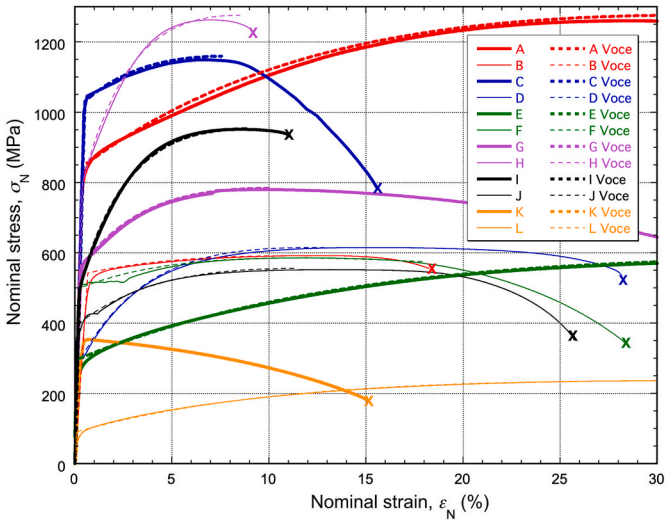

Fig. 3. Nominal stress – nominal strain curves for all of the (12) materials, derived both directly from tensile testing and in the form of the (best-fit) Voce sets shown in Table 3 which have been converted to nominal form using Eqns. (6) and (7). The Voce-based curves are shown only up to the onset of necking (peak in the plot).

Table 3
Sets of Voce parameter values giving optimised fit with tensile stress-strain curves. Also shown are corresponding values of the UTS.

Metal Code	Voce parameter values (best fit with tensile data)			Ultimate Tensile Stress σ_{UTS} (MPa)
	Yield stress σ_Y (MPa)	Saturation stress, σ_s (MPa)	Characteristic strain, ε_0 (%)	
A	846	2103	25.2	1275
B	542	717	10.0	590
C	1030	1302	4.6	1159
D	282	715	4.1	613
E	297	1068	30.1	574
F	500	698	7.5	574
G	555	896	4.2	783
H	800	1421	2.8	1276
I	500	1100	2.8	952
J	398	652	5.3	555
K	350	400	14.3	350
L	60	360	16.2	235

For example, none of them exhibit "premature" (pre-necking) fracture - this would occur before the peak of a nominal stress – nominal strain curve. Also, none of them exhibit any "anomalous" features, such as strongly "transitional" yielding (possibly excepting L), strain bursting/Lüders plateaux (excepting very minor features in F and J) or sigmoidal shapes. These Voce-defined true stress-strain curves can thus be used with confidence in modelling the behaviour of these materials (up to large plastic strains).

For most materials, comparing modelled and experimental (nominal) stress-strain curves up to the onset of necking is an acceptably accurate way of establishing the best fit Voce set. However, for materials that exhibit little or no work hardening, and hence neck at very low strains – such as K (as-received copper) in the current set, this might be rather inaccurate. One way to improve the reliability of the inferred Voce set is to extend the comparison up into the post-necking regime, which requires an FEM model to be set up with the specific geometry of the tensile test-piece. The outcome of this operation for material K is presented in Fig. 4, which shows both a comparison between measured and (best fit) modelled curves (up to fracture) and the plastic strain field at the point of rupture. The peak (true) strain in the neck at this point is about 100%, which is a typical figure for a critical (true) plastic strain at fracture (and is a more meaningful parameter than the nominal value at this point – i.e. the "ductility", which depends on sample dimensions, but is usually far below the true strain at rupture – it's about 15% for the test concerned).

3.2. Vickers hardness testing

3.2.1. Hardness data and inferred YS and UTS values

The experimental hardness test data are shown in Table 4. Each measured value of d is the average from 5 indents (taking both diagonals in each case), with an approximate indication of the standard deviation (and corresponding variations in H_V) also given. This table also includes the values of YS and UTS obtained using Eqns. (1) and (2), with the parameter values proposed by Pavlina and Van Tyne (for all non-

Table 4
Vickers test outcomes, for an applied load of 10 kg. H_V was obtained from measured indent diagonals (d), using Eqn. (4). The YS and UTS values were obtained using Eqns. (1) and (2), using the values of A, a, C and c in Table 1, as proposed by Pavlina & Van Tyne or by Umemoto et al. These are shown only for the materials falling into the categories concerned – see Table 1.

Metal Code	Hardness parameters		Pavlina & Van Tyne		Umemoto et al.	
	Average diagonal, d (μm)	Hardness, H_V (kg mm^{-2})	YS (MPa)	UTS (MPa)	YS (MPa)	UTS (MPa)
A	226 ± 4	360 ± 10				
B	309 ± 2	193 ± 3				
C	232 ± 1	342 ± 2	896	1190	(iv) 632	(iv) 1089
D	328 ± 7	173 ± 10	408	553	(ii) 346	(ii) 519
E	368 ± 5	137 ± 6				
F	308 ± 4	195 ± 5	472	634	(i) 330	(i) 482
G	280 ± 2	236 ± 5	590	790	(ii) 472	(ii) 708
H	228 ± 4	356 ± 6	936	1243	(ii) 713	(ii) 1068
I	265 ± 6	264 ± 7	671	896	(ii) 529	(ii) 792
J	321 ± 3	176 ± 2	417	564	(i) 298	(i) 435
K	425 ± 15	102 ± 4				
L	530 ± 20	66 ± 4				

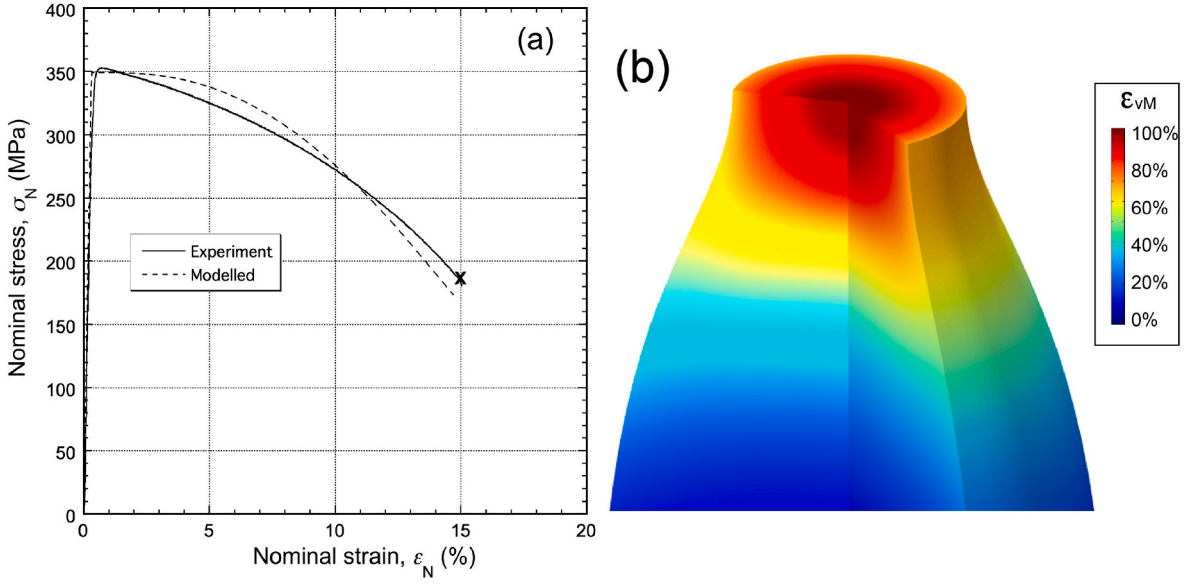

Fig. 4. (A) Measured and (best fit) modelled nominal stress-strain curves for material K and (b) modelled (von Mises) strain field at the (experimental) point of fracture. The Voce set used was that listed for material K in Table 3. The test-piece was cylindrical, having a gauge section 25 mm long, with a diameter of 5 mm.

austenitic, hypoeutectoid steels) and by Umemoto et al. (for (i) ferritic, (ii) pearlitic and (iv) martensitic steels, which all fall within that category).

These predicted values of YS and UTS can be compared with those in Table 3, which are from the tensile testing. It is clear just from this very limited comparison that the predictive power of these empirical relationships is limited. While some of the predictions are close, others are in error by large factors. Taking a single example, for alloy C (a martensitic steel), with a measured H_V of 342, the inferred YS is about 900 MPa from Pavlina & Van Tyne and about 630 MPa from Umemoto et al. (version for martensitic steels), whereas the actual YS (from tensile testing) is about 1030 MPa. On the other hand, the UTS values are mostly quite close, particularly for the Pavlina & Van Tyne expression.

3.2.2. *Modelling of the Vickers test*

Since the stress-strain curves have already been established by tensile testing, and captured as sets of Voce parameter values (Table 2), these Vickers tests can be simulated, using the FEM model described in §2.3.2. The outcome of this, in terms of the residual indent shape, is shown in Fig. 5. Also shown in this figure are the values of $d/2$ expected to be obtained in the test (taken as the distance from the indentation axis to the highest point in the pile-up) and the corresponding H_V values.

These predicted H_V values are plotted in Fig. 6 against the directly-measured values. There is clearly a large degree of correlation, although with some scatter and an apparent tendency for the measured values to be slightly below the modelled ones. Such uncertainties, and possibly a trend of some sort, constitute a potential source of "error" in obtaining a hardness number, which is quite separate from those arising when attempting to convert a hardness number to a YS or UTS. It could, however, be argued that this is unimportant, since a hardness number has no intrinsic significance (and any systematic deviation from a "theoretical" value will be incorporated into an empirical correlation with tensile test data).

3.3. *PIP testing*

In all cases, the indents were found to be radially symmetric, which is consistent with these materials all being at least approximately isotropic. The best fit Voce parameter values are shown in Table 5. Excellent fits between measured and modelled profiles were obtained in all cases. Two example comparisons are shown in Fig. 7. It may be noted that the (automated) PIP procedure involves selection of the load to create a penetration ratio (δ/R) in a suitable range – usually between 10% and 20%. In these two cases, the load was substantially higher for the Ni superalloy (A) than for the Al alloy (B).

A comparison between measured (nominal) stress-strain curves, as obtained by tensile testing and by using the PIP procedure, is shown in

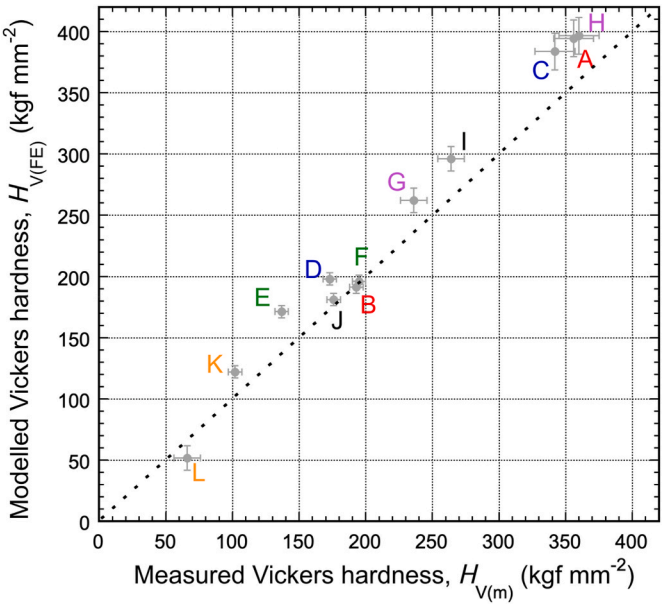

Fig. 6. Comparison between the Vickers hardness numbers obtained by direct measurement and by FEM simulation of the test (using the Voce parameter sets in Table 3).

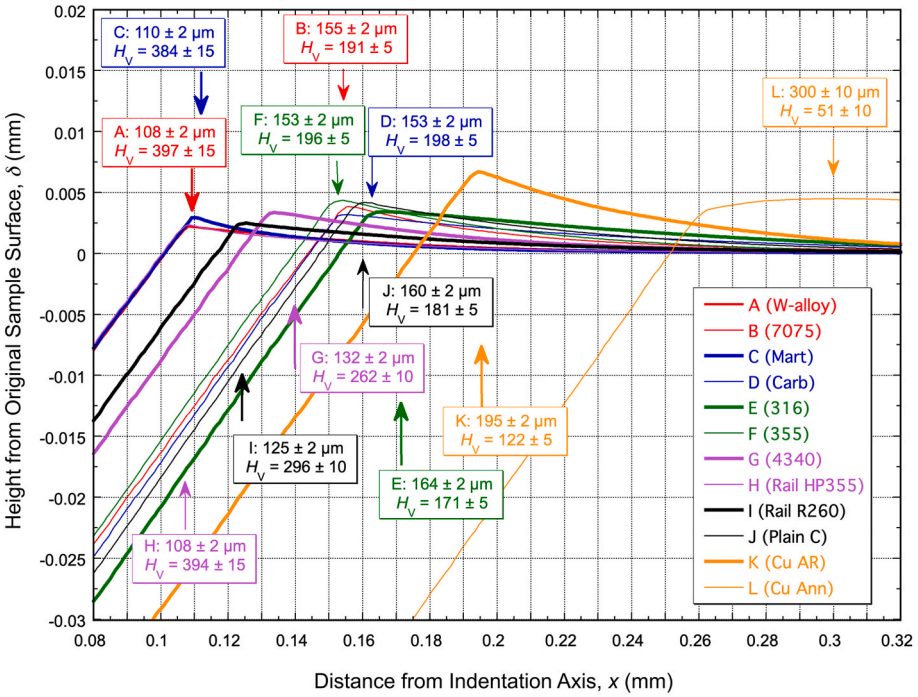

Fig. 5. FEM model predictions for the indent profiles (along a diagonal) after Vickers hardness testing (with a load of 10 kg), obtained using the Voce parameter sets in Table 3. Shown in the boxes are the expected values of $d/2$ and corresponding inferred H_V values, obtained using Eqn. (4).

Table 5
PIP outcomes in the form of sets of Voce parameters, and corresponding UTS values.

Code	Best fit Voce parameter values			Ultimate Tensile Stress σ_{UTS} (MPa)
	Yield stress σ_Y (MPa)	Saturation stress, σ_s (MPa)	Characteristic strain, ε_0 (%)	
A	819	1559	8.8	1225
B	550	703	9.5	589
C	974	1343	9.5	1100
D	311	782	6.3	636
E	225	743	10.0	551
F	453	718	8.9	585
G	577	898	6.8	747
H	795	1528	4.3	1318
I				
I	541	1226	6.3	1001
J	402	801	14.0	577
K	314	358	6.1	322
L	41	250	7.1	195

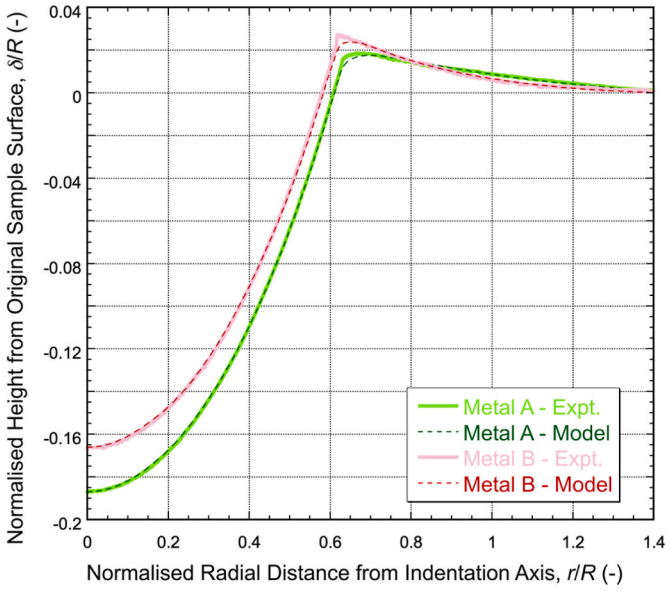

Fig. 7. Comparison between modelled and measured PIP indent profiles, for A (Waspalloy) and B (7075 Al).

Fig. 8. While the Voce parameter sets in Table 3 (directly fitted to tensile data) and Table 5 (PIP-derived) are not identical, it can be seen in this figure that the level of agreement between PIP-derived and directly-measured tensile curves is good. In fact, similar levels of agreement have been found many times before. Data extracted from these curves are plotted in Fig. 9, in the form of PIP-derived against tensile-derived values of YS and UTS. The correlation is close, although it is always recommended that complete stress-strain curves should be compared. This is a more demanding and reliable kind of assessment (eliminating potential errors from variations in how the YS is defined, or from the yielding being strongly transitional). Just to give a single example of this, while the PIP-derived YS for metal L is well-defined (at about 40 MPa), the corresponding value from the tensile test could be anywhere between this and about 80 MPa, depending on the construction used to obtain it. A value of about 60 MPa was obtained here, using the 0.2% offset procedure. In any event, there are certainly no substantial discrepancies here between any of the tensile curves and corresponding PIP-derived ones.

Just to complete this comparison, the information in Fig. 8 has been replotted in Fig. 10, in the form of true stress-strain curves. For the PIP data, this is straightforward, since these curves are just plots of the Voce law (with the optimised parameter values, shown in Table 5). For the tensile plots, the raw data are the nominal stress-strain curves, although these can be used only up to the peak (onset of necking). This presents a problem for the metals, such as K, that neck at very low strains. However, this problem has already been addressed in constructing Fig. 3, so the true curves for the tensile plots in Fig. 10 are Voce plots based on the parameter values in Table 3. (Since these are just plots of the Voce equation, they are shown as a function of the plastic strain and hence do not start at the origin.) This plot gives a clearer indication of the true work hardening behaviour exhibited by each of these metals, which cover a very wide range.

4. Relation between hardness number and stress-strain curve

4.1. Use of empirical relationships

A comparison is shown in Fig. 11 between YS and UTS values from tensile testing and those obtained from measured H_V values via the parameter values of Pavlina & Van Tyne (YS and UTS), Tabor (YS only) and the BS ISO-18265:2013 standard (UTS only). This has been done for all of the materials. Recognizing that these equations are being applied to a wider range of metals than those for which they were proposed, and also that this is a small data set, these comparisons do indicate that only limited confidence can be placed in H_V-derived values obtained in this way. This applies particularly to YS values. For UTS estimation, on the other hand, both the Pavlina & Van Tyne equation and the BS standard expression are reasonably accurate (with P&VT apparently slightly better for the harder metals and BS better for the softer ones). It is, however, clear that YS values obtained in this way are much less reliable – errors of up to about 30% are observed. There is thus little or no reliable information concerning the shape of the curve, or even the uniform elongation (necking strain), so there are no clear indications about work hardening rates. Such information is essential if the mechanical response of the material in various loading configurations is to be quantitatively predicted.

4.2. Sources of error

It might be argued that the approach of using different expressions for different classes (or sub-classes) of metal should be taken down to a finer level of detail (alloy composition, prior thermo-mechanical treatment etc), rather than applied universally in this way. In practice, a procedure of this type only has potential value if expressions can be used that are universally applicable – or at least are confined only to very broad classes of metal type (and are reliable within those limitations).

A clear message from Fig. 11 is that the errors tend to be larger for materials that exhibit pronounced work hardening (and hence have a large difference between the YS and UTS values). This is expected, since, as outlined in the introduction, and originally suggested by Tabor, a simple linear dependence of the YS on H_V, with the factor relating them being close to 3, is expected in the complete absence of work hardening. This works quite well in the present set for metals B, C and K. Unfortunately, without prior knowledge that work hardening is negligible, this is of little practical use. Furthermore, even for a particular type of metal, the degree of work hardening it exhibits can depend quite strongly on the thermo-mechanical treatment that it has received – this can be highlighted by comparing metals K and L. On the other hand, the correlations do tend to be more reliable if the focus is on the UTS. It is difficult to establish exactly why this is the case, although it is worth noting that a UTS value is the outcome of both yielding and work hardening characteristics (whereas the YS has no sensitivity to work hardening).

Finally, some insights can be obtained by study of strain fields typically generated during Vickers and PIP testing. Those after Vickers testing are shown in Fig. 12 for metal K (initially harder, but with little

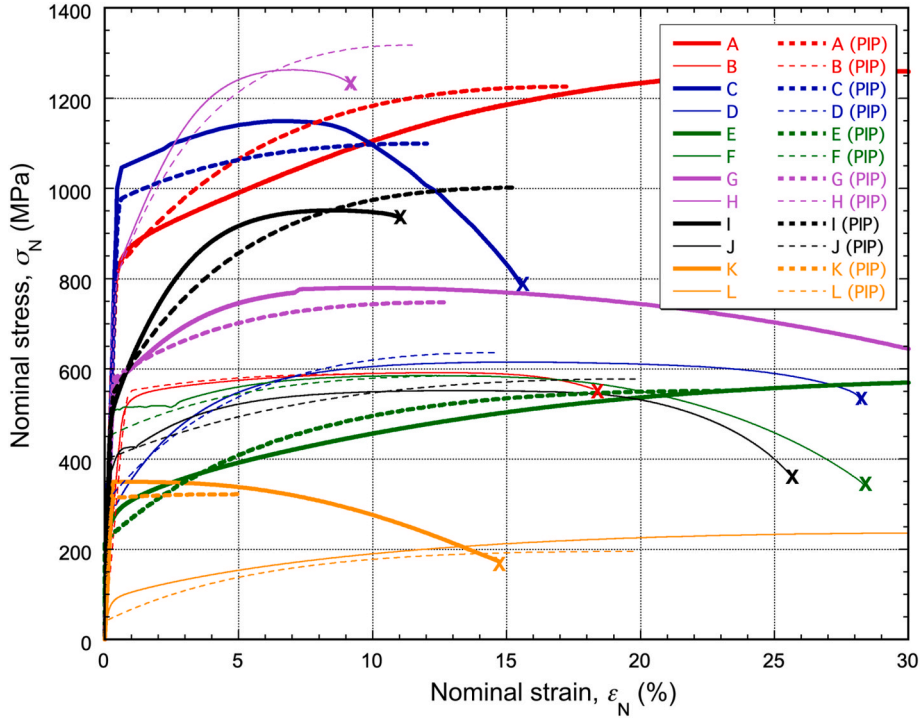

Fig. 8. Nominal stress – nominal strain curves for all of the materials, from tensile testing and from PIP (Voce sets shown in Table 5, converted to nominal form using the standard analytical relationships). The latter are shown only up to the onset of necking (peak in the plot).

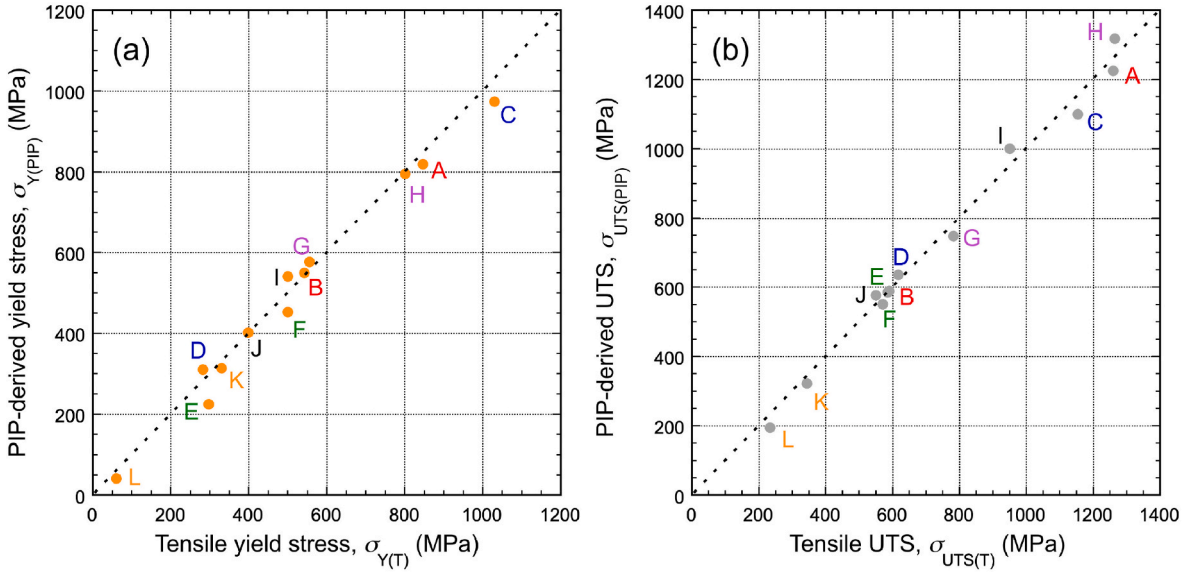

Fig. 9. Comparison between (a) YS and (b) UTS values extracted from tensile curves and obtained via PIP testing.

work hardening) and metal L (initially softer, but with strong work hardening). In view of the lack of radial symmetry, sections are shown both parallel to the long diagonal and normal to the side of the pyramid. In both cases, very high (true) strains are generated (up to 200%), but they occur only in very small volumes (near to the apex). One of the problems (which becomes even more severe during most "nano-indentation") is that the overall response is likely to be sensitive to local microstructural effects – unless the grain size is exceptionally small, the regions in which these very high strain gradients are being generated will be below the scale of the individual grains and hence will tend to have a different response from that of the bulk. Furthermore, apart from this very thin region close to the indenter, strain levels in most of the sample are low. This tends to have the effect that the overall response, and particularly the indent diagonal – which is the only measured outcome, is not very sensitive to the work hardening characteristics. This is reflected in the poor sensitivity to detection of the significance of work hardening.

Corresponding plastic strain fields after PIP testing are shown in Fig. 13, with the radial symmetry allowing just single sections to be shown in each case. Several differences from the Vickers strain fields are apparent. An obvious one is that the scale of the region being deformed is much greater – note the different scale bars, capturing the bulk response much more reliably. Another is that, while peak strains are lower, strains in the range of primary interest (up to a few tens of %) are

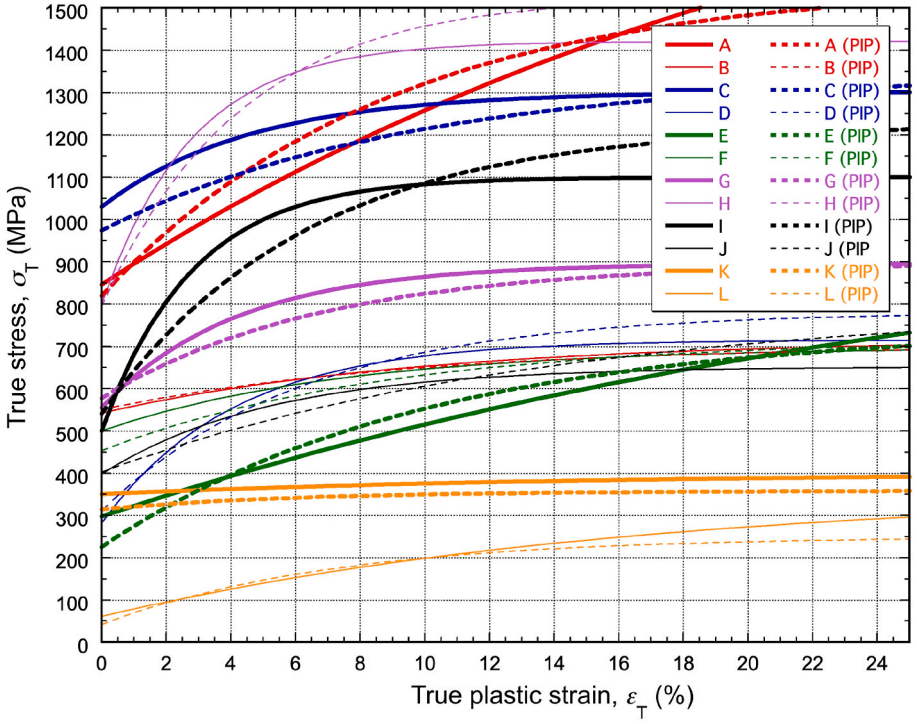

Fig. 10. True stress – true strain curves for all of the materials, obtained from tensile testing and from PIP.

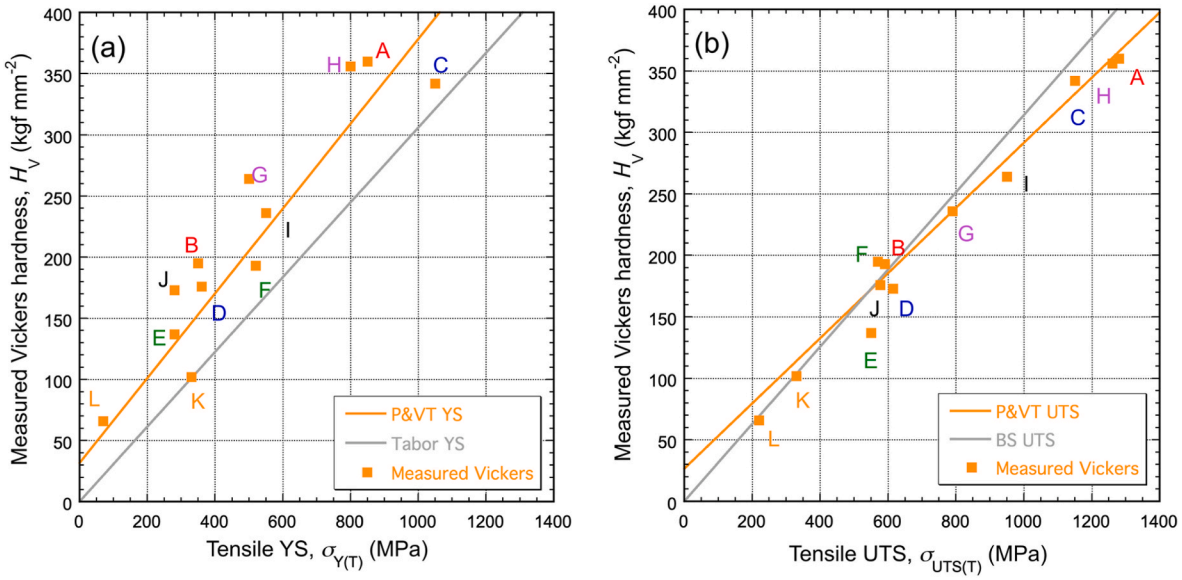

Fig. 11. Plot of (a) YS and (b) UTS values from experimental H_V values against corresponding tensile tests. Also shown are plots of the relationship of Pavlina & Van Tyne, the simple (Tabor) expression of YS = UTS = $H_V/3$ (expected to apply in the complete absence of work hardening) and the BS standard for UTS (Eqn. (3)).

being "diffused" over much larger volumes, with the strain field thus having a much greater sensitivity to the work hardening characteristics: higher work hardening rates (metal L) tend to cause the strains to become more diffuse, with the peak values being lower. The pile-up height is also very sensitive to the strength of the work hardening - it is much greater with materials that exhibit little work hardening (K). This point has been clearly recognised since the pioneering work of Hill et al. (1989), which incorporated finite element modelling of the Brinell test. Since the experimental measurements cover the complete shape of the indent profile (rather than just the length of a diagonal), the final outcome is very sensitive to the work hardening characteristics – ie to the actual shape of the stress-strain curve.

Although these features do not constitute the only differences between the procedures involved in PIP and hardness testing, they are part of the explanation for the differences between the outcomes obtained with the two procedures.

5. Conclusions

This work concerns the use of two indentation-based test procedures to infer features of the (nominal) stress-strain curve, as obtained via conventional tensile testing. Experimental data have been obtained for

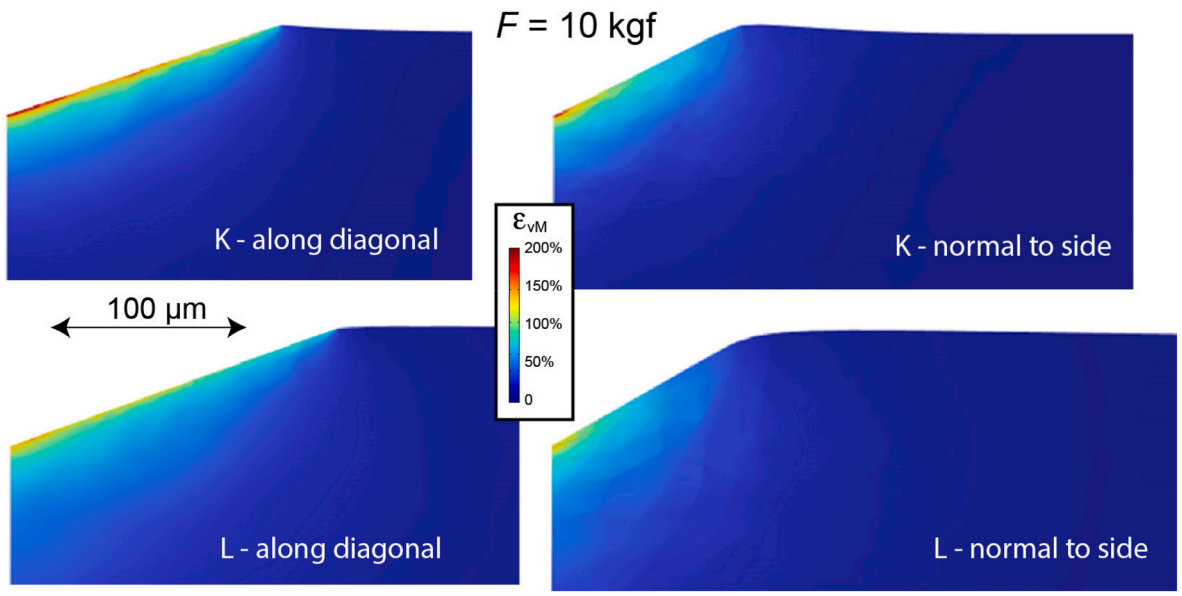

Fig. 12. Fields of equivalent (von Mises) plastic strain after carrying out a Vickers test, with a load of 10 kgf, on materials K and L.

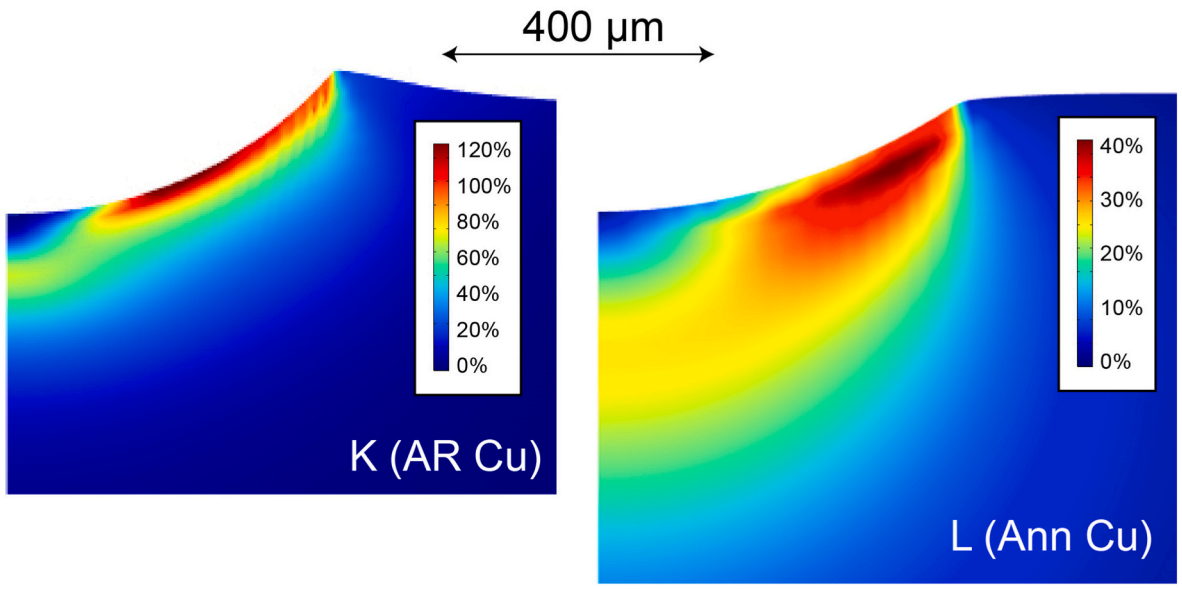

Fig. 13. Fields of (von Mises) plastic strain after PIP testing of materials K and L. The loads were selected to give similar penetration depths (~180 μm, corresponding to a penetration ratio of ~18%) in both cases.

12 different alloys, selected to cover a wide range of curve shapes and characteristics. While the statistical significance of the data is therefore rather limited, an attempt has been made to explore the relationship between underlying plasticity characteristics and experimental outcomes of these tests. The following points have been investigated and established.

1) While hardness numbers can provide useful (semi-quantitative) indicators of the resistance to plastic deformation, using them (via empirical correlations) to obtain parameters related to the complete nominal stress-strain curve – notably the YS and UTS – can be subject to relatively large errors. These arise primarily from effects caused by work hardening, with hardness test outcomes having a low sensitivity to its nature.
2) If the focus is restricted to the UTS, and to certain types of alloy (such as ferritic/pearlitic/martensitic steels), then hardness-derived data are likely to be much more reliable. If the objective is indeed simply to obtain UTS values, then continued use of hardness testing can be justified.
3) It should, however, be noted that the UTS is a nominal stress that has meaning only in the context of uniaxial tensile testing. It carries no information about the onset of yielding or about any features of the true stress-strain curve - which is essential for prediction of how any component or structure will respond to loading that might promote inelastic behaviour. Some insights are offered here into details of the errors that are likely to arise when processing hardness numbers via empirical correlations.
4) In contrast to this, the immediate experimental outcome of a PIP test is the complete indentation profile, which potentially carries detailed quantitative information about the work hardening characteristics. These characteristics, as well as the yield stress, are automatically extracted from the profile via iterative FEM simulation

of the progression of the test. It is shown that this leads, not only to reliable YS and UTS values, but also to the complete (true) stress-strain curve.

Author statement

This paper presents a systematic comparison, for 12 different alloys, between information obtained via tensile testing, hardness testing and PIP (Profilometry-based Indentation Plastometry) testing. This resubmitted version has been modified in accordance with reviewer comments and suggestions.

Declaration of competing interest

The authors declare that they have no known competing financial interests or personal relationships that could have appeared to influence the work reported in this paper.

Data availability

Data will be made available on request.

Acknowledgements

Financial support is acknowledged from EPSRC, via Grant No. EP/I038691/1. Relevant support has also been received from the Leverhulme Trust, in the form of an International Network grant (IN-2016-004) and an Emeritus Fellowship (EM/2019–038/4). In addition, an ongoing Innovate UK grant (project number 10006185) covers work in this area and JEC is in receipt of a Future Leaders grant from Innovate UK (MR/W01338*X*/1), which is focussed on PIP usage.

This publication, and the work it describes, were supported by the Health and Safety Executive (HSE). Its contents, including any opinions and/or conclusions expressed, are those of the authors alone and do not necessarily reflect HSE policy.

References

Branch, N.A., Subhash, G., Arakere, N.K., Ma, Klecka, 2010. Material-dependent representative plastic strain for the prediction of indentation hardness. Acta Mater. 58, 6487. https://doi.org/10.1016/j.actamat.2010.08.010.

Burley, M., Campbell, J.E., Reiff-Musgrove, R., Clyne, J.Dean & TW., 2021. The effect of residual stresses on stress–strain curves obtained via profilometry-based inverse finite element method indentation plastometry. Adv. Eng. Mats., 2001478 https://doi.org/10.1002/adem.202001478.

Busby, J.T., Hash, M.C., Was, G.S., 2005. The relationship between hardness and yield stress in irradiated austenitic and ferritic steels. J. Nucl. Mats. 336 https://doi.org/10.1016/j.jnucmat.2004.09.024, 267.

Campbell, J.E., Thompson, R.P., Dean, J., Clyne, T.W., 2018. Experimental and computational issues for automated extraction of plasticity parameters from spherical indentation. Mech. Mater. 124, 118. https://doi.org/10.1016/j.mechmat.2018.06.004.

Campbell, J.E., Thompson, R.P., Dean, J., Clyne, T.W., 2019. Comparison between stress-strain plots obtained from indentation plastometry, based on residual indent profiles, and from uniaxial testing. Acta Mater. 168, 87. https://doi.org/10.1016/j.actamat.2019.02.006.

Campbell, J.E., Gaiser-Porter, M., Gu, W., Ooi, S., Burley, M., Dean, J., Clyne, T.W., 2022. Indentation plastometry of very hard metals. Adv. Eng. Mats., 2101398 https://doi.org/10.1002/adem.202101398.

Chakraborty, A., Eisenlohr, P., 2017. Evaluation of an inverse methodology for estimating constitutive parameters in face-centered cubic materials from single crystal indentations. Europ. J. Mech. A 66, 114. https://doi.org/10.1016/j.euromechsol.2017.06.012.

Chen, H., Cai, L.X., 2018. Theoretical conversions of different hardness and tensile strength for ductile materials based on stress-strain curves. Metall. Mater. Trans. 49A, 1090. https://doi.org/10.1007/s11661-018-4468-8.

Clyne, T.W., Campbell, J.E., 2021. Testing of the Plastic Deformation of Metals. Cambridge University Press, Cambridge, U.K.. https://doi.org/10.1017/9781108943369

Clyne, T.W., Campbell, J.E., Burley, M., Dean, J., 2021. Profilometry-based inverse FEM indentation plastometry (PIP). Adv. Eng. Mats., 21004037 https://doi.org/10.1002/adem.202100437.

Dean, J., Clyne, T.W., 2017. Extraction of plasticity parameters from a single test using a spherical indenter and FEM modelling. Mech. Mater. 105, 112. https://doi.org/10.1016/j.mechmat.2016.11.014.

Dean, J., Wheeler, J.M., Clyne, T.W., 2010. Use of quasi-static nanoindentation data to obtain stress-strain characteristics for metallic materials. Acta Mater. 58, 3613. https://doi.org/10.1016/j.actamat.2010.02.031.

Frydrych, K., Papanikolaou, S., 2022. Unambiguous identification of crystal plasticity parameters from spherical indentation. Crystals 12. https://doi.org/10.3390/cryst12101341.

Gu, W., Campbell, J.E., Tang, Y.T., Safaie, H., Johnston, R., Gu, Y., Pleydell-Pearce, C., Burley, M., Dean, J., Clyne, T.W., 2022. Indentation plastometry of welds. Adv. Eng. Mats., 2101645 https://doi.org/10.1002/adem.202101645.

Hashemi, S.H., 2011. Strength-hardness statistical correlation in API X65 steel. Mater. Sci. Eng. 528, 1648. https://doi.org/10.1016/j.msea.2010.10.089.

Heinrich, C., Waas, A.M., Wineman, A.S., 2009. Determination of material properties using nanoindentation and multiple indenter tips. Int. J. Solid Struct. 46, 364. https://doi.org/10.1016/j.ijsolstr.2008.08.042.

Hill, R., Storakers, B., Zdunek, A.B., 1989. A theoretical study of the Brinell hardness test. Proc. Roy. Soc. Lond. A 423, 301. https://doi.org/10.1098/rspa.1989.0056.

Kucharski, S., Mroz, Z., 2007. Identification of yield stress and plastic hardening parameters from a spherical indentation test. Int. J. Mech. Sci. 49, 1238. https://doi.org/10.1016/j.ijmecsci.2007.03.013.

Lee, J., Lee, C., Kim, B., 2009. Reverse analysis of nano-indentation using different representative strains and residual indentation profiles. Mater. Des. 30, 3395. https://doi.org/10.1016/j.matdes.2009.03.030.

Matyunin, V.M., Marchenkov, A.Y., Agafonov, R.Y., Danilin, V.V., Ma, Karimbekov, Goryachkina, M.V., Volkov, P.V., Zhgut, D.A., 2021. Correlation between the Ultimate Tensile Strength and the Brinell Hardness of Ferrous and Nonferrous Structural Materials. Russian Metallurgy, 2021, p. 1719. https://doi.org/10.1134/s0036029521130164.

Meng, L., Breitkopf, P., Raghavan, B., Mauvoisin, G., Bartier, O., Hernot, X., 2019. On the study of mystical materials identified by indentation on power law and Voce hardening solids. Int. J. Material Form. 12, 587. https://doi.org/10.1007/s12289-018-1436-1.

Ooi, S., Reiff-Musgrove, R., Gaiser-Porter, M., Steinbacher, M., Griffin, I., Campbell, J.E., Burley, M., Warwick, C.M., Vaka, H., Clyne, T.W., 2022. PIP testing for characterization of case hardened steels. Adv. Eng. Mats., 2201512 https://doi.org/10.1002/adem.202201512.

Patel, D.K., Kalidindi, S.R., 2016. Correlation of spherical nanoindentation stress-strain curves to simple compression stress-strain curves for elastic-plastic isotropic materials using finite element models. Acta Mater. 112, 295. https://doi.org/10.1016/j.actamat.2016.04.034.

Pavlina, E.J., Van Tyne, C.J., 2008. Correlation of yield strength and tensile strength with hardness for steels. J. Mats. Eng. & Performance 17. https://doi.org/10.1007/s11665-008-9225-5, 888.

Pintaude, G., 2022. Hardness as an indicator of material strength: a critical review. Crit. Rev. Solid State Mater. Sci. https://doi.org/10.1080/10408436.2022.2085659.

Reiff-Musgrove, R., Gu, W., Campbell, J.E., Reidy, J., Bose, A., Chitrapur, A., Tang, Y.T., Burley, M., Clyne, T.W., 2022. Effect of relatively low levels of porosity on the plasticity of metals and implications for profilometry-based indentation plastometry (PIP). Adv. Eng. Mats. https://doi.org/10.1002/adem.202200642.

Reiff-Musgrove, R., Gaiser-Porter, M., Gu, W., Campbell, J.E., Lewis, P., Frehn, A., Tarrant, A.D., Tang, Y.T., Burley, M., Clyne, T.W., 2023. Indentation plastometry of particulate metal matrix composites, highlighting effects of microstructural scale. Adv. Eng. Mater. https://doi.org/10.1002/adem.202201479.

Sandomirskii, S.G., 2017. Estimation of the Ultimate Tensile Strength of Steel from its HB and HV Hardness Numbers and Coercive Force. Russian Metallurgy, p. 989. https://doi.org/10.1134/s003602951711012x.

Southern, T., Campbell, J.E., Kourousis, K.I., Mooney, B., Tang, Y.T., Clyne, T.W., 2023. Indentation plastometry for study of anisotropy and inhomogeneity in maraging steel produced by laser powder bed fusion. Steel Res. Int. https://doi.org/10.1002/srin.202200881.

Tabor, D., 1948. A simple theory of static and dynamic hardness. Proc. Roy. Soc. A 192, 247. https://doi.org/10.1098/rspa.1948.0008.

Tabor, D., 1996. Indentation Hardness: fifty years on. A personal view. Phil. Mag. 74, 1207. https://doi.org/10.1080/01418619608239720.

Tang, Y.T., Campbell, J.E., Burley, M., Dean, J., Reed, R.C., Clyne, T.W., 2021. Use of profilometry-based indentation plastometry to obtain stress-strain curves from anisotropic superalloy components made by additive manufacturing. Materialia 15, 101017. https://doi.org/10.2139/ssrn.3746800.

Tekkaya, A.E., 2001. Improved relationship between Vickers hardness and yield stress for cold formed materials. Steel Res. 72 https://doi.org/10.1002/srin.200100122, 304.

Tiryakioglu, M., 2015. On the relationship between Vickers hardness and yield stress in Al-Zn-Mg-Cu Alloys. Mater. Sci. Eng. 633 https://doi.org/10.1016/j.msea.2015.02.073, 17.

Umemoto, M., Liu, Z.G., Tsuchiya, K., Sugimoto, S., Bepari, M.M.A., 2001. Relationship between hardness and tensile properties in various single structured steels. Mater. Sci. Technol. 17 https://doi.org/10.1179/026708301101510339, 505.

Wang, M.Z., Wu, J.J., Hui, Y., Zhang, Z.K., Zhan, X.P., Guo, R.C., 2017. Identification of elastic-plastic properties of metal materials by using the residual imprint of spherical indentation. Mater. Sci. Eng. 679, 143. https://doi.org/10.1016/j.msea.2016.10.025.

Warwick, M., Vaka, H., Fang, C.Z., Campbell, J., Dean, J., Clyne, T.W., 2023. Use of profilometry-based indentation plastometry to study the effects of pipe wall

flattening on tensile stress-strain curves of steels. Steel Res. Int. 94. https://doi.org/10.1002/srin.202200920.

Xue, H., He, J.X., Jia, W.N., Zhang, J.L., Wang, S., Zhang, S., Yang, H.L., Wang, Z., 2020. An approach for obtaining mechanical property of austenitic stainless steel by using continuous indentation test analysis. Structures 28, 2752. https://doi.org/10.1016/j.istruc.2020.11.001.

Yao, W.Z., Krill, C.E., Albinski, B., Schneider, H.C., You, J.H., 2014. Plastic material parameters and plastic anisotropy of tungsten single crystal: a spherical micro-indentation study. J. Mater. Sci. 49, 3705. https://doi.org/10.1007/s10853-014-8080-z.

Zhang, C.Y., Li, F.X., Wang, B., 2013. Estimation of the elasto-plastic properties of metallic materials from micro-hardness measurements. J. Math. Sci. 48, 4446. https://doi.org/10.1007/s10853-013-7263-3.